Online-Journals.org

iJOE International Journal of Online and Biomedical Engineering

iJOE | eISSN: 2626-8493 | Vol. 19 No. 14 (2023) | OPEN ACCESS

https://doi.org/10.3991/ijoe.v19i14.42163

PAPER

Diagnosis of Osteoporosis Using Transfer Learning in the Same Domain

Abulkareem Z. Mohammed[1](✉), Loay E. George[2]

[1]Informatics Institute for Postgraduate Studies, Baghdad, Iraq

[2]College of Science, Baghdad University, Baghdad, Iraq

phd202010550@iips.icci.edu.iq

ABSTRACT

This paper presents a system for diagnosing osteoporosis using x-rays by leveraging transfer learning in the same domain. The proposed system consists of phase 1 and phase 2; each phase includes several stages, as the pre-processing stage appropriately prepares the source image via noise reduction by the average filter, contrast enhancement using histogram equalization, and obtaining the region of interest by employing K-mean and edge detection, followed by the smudging stage through a mean filter with a large window size, which subsequently contributed to facilitating the diagnosis. The stages mentioned in both phases are similar. In phase 1, the model is trained on a large unlabeled x-ray dataset collected from different orthopedic centers to identify the general features of the image. In phase 2, fine-tune the trained model with the target dataset; this approach is beneficial when the target task has limited labeled data or when training a model from scratch is computationally expensive. It is worth noting that two datasets were used as target datasets. The accuracy of diagnosing osteoporosis using the proposed deep convolutional neural network (DCNN) model was 94.5 with the osteoporosis knee x-ray database (Dataset A). The accuracy of diagnosing osteoporosis using transfer learning in the same field was 98.91 when training the proposed DCNN model with a large unlabeled dataset and fine-tuning with the target database, osteoporosis knee x-ray database (Dataset A). The accuracy of diagnosing osteoporosis using the proposed DCNN model was 91.5 with the knee x-ray osteoporosis database (Dataset B). The accuracy of diagnosing osteoporosis using transfer learning in the same field was 96.61 when training the proposed DCNN model with a large unlabeled dataset and fine-tuning with the target knee x-ray osteoporosis database (Dataset B).

KEYWORDS

osteoporosis detection, x-ray, deep convolutional neural network (DCNN), smudging, transfer learning

1 INTRODUCTION

Osteoporosis is a medical condition in which bones become fragile and brittle, leading to an increased risk of fractures, especially of the hip, spine, and wrist [1–3].

Mohammed, A.Z., George, L.E. (2023). Diagnosis of Osteoporosis Using Transfer Learning in the Same Domain. *International Journal of Online and Biomedical Engineering (iJOE)*, 19(14), pp. 142–159. https://doi.org/10.3991/ijoe.v19i14.42163

Article submitted 2023-06-10. Revision uploaded 2023-06-28. Final acceptance 2023-06-29.

This condition occurs due to the gradual loss of bone density and mass, making the bones weak and susceptible to fractures [4] [5]. Osteoporosis is a highly prevalent condition affecting millions worldwide, with postmenopausal women being particularly vulnerable [6] [7]. Factors that increase the risk of osteoporosis include advancing age, family history, inadequate calcium intake, and a sedentary lifestyle. The condition can be prevented and treated with lifestyle changes and medications [8].

Osteoporosis detection typically involves a combination of medical history evaluation, physical examination, and imaging tests such as magnetic resonance imaging (MRI), computerized tomography (CT), and dual x-ray absorptiometry (DEXA or DXA) [9] [10]. Through this, the bone mineral density is measured and compared with predefined values (threshold), and according to the result, the case is diagnosed as having osteoporosis or normal.

X-rays are also used to assess the cortical bone, which is "the hard outer layer of bone that surrounds the internal cavity to provide protection," and it is known for its high resistance to bending and torsion. Cortical bone, also referred to as compact bone, constitutes approximately 80% of the skeletal mass and plays a vital role in maintaining body structure and supporting weight-bearing [11]. Trauma or a bone condition such as osteoporosis can harm the cortical bone in the spine, arms, and legs. The primary objective of osteoporosis detection is to identify individuals at risk of fractures and promptly initiate preventive treatment [12–14].

Many computer-based systems are used to diagnose medical images, whether for osteoporosis, arthritis, cancer, etc. Some of these systems are based on traditional methods; others use deep learning [15–18], and some studies use transfer learning to diagnose medical images [19–22].

The body area most targeted for diagnosing osteoporosis is the spine using DEXA scans and the knee bone using x-rays. This work relied on x-rays due to their availability and low cost. This paper addressed several issues, including the low accuracy of osteoporosis detection, which is primarily caused by the difficulty in distinguishing between the osteoporotic and normal images. This problem was overcome by using the smudging method. Another problem is the need for more available datasets in this field, which was overcome using transfer learning in the same domain.

2 RELATED WORK

There are several previous works dealing with osteoporosis detection, including S. C. Radominski et al. [23], which extracted the trabecular bone texture characteristics from MRI images to examine the quantitative value of high-resolution MRI in femoral microstructures and discovered that the majority of the texture parameters were statistically different.

N. Tomita et al. [24] suggested using DCNN to find osteoporotic vertebral fractures (VF). After using computed tomography scans of vertebrae to extract logical features, the system's performance was compared to that of working radiologists, and similar outcomes were obtained.

I. Bortone et al. [25] provided a supervised method based on an experimental non-invasive analysis of static and dynamic BMD measurements to categorize the BMD state of postmenopausal women. The study shows the value of using machine

learning techniques such as ANNs and SVMs to investigate the association between women's BMD and static and dynamic baropodometry.

J. S. Lee et al. [26] used dental panoramic radiographs and a convolutional neural network (CNN) to identify osteoporosis in the tooth. This DCNN outperformed the outcomes of oral and maxillofacial radiologists. The outcomes of the model reflect a very good 92.5 without data augmentation.

J. Liu et al. [27] discussed using x-rays of the pelvis to diagnose osteoporosis. They derived the energy function from the Soft Max of the suggested U-Net model, which utilizes x-rays to detect osteoporosis by analyzing the deep features of the medullary joint. The photos of the bone mass decrease group and the osteoporosis group in this investigation need to be more adequately diagnosed.

Tecle et al. [28] utilized the Alex Net Classifier to evaluate osteoporosis diagnoses. They utilized x-ray images of the hand and classified the segmented images of the second metacarpal region into osteoporotic and non-osteoporotic groups.

S. Lee et al. [29] evaluated the use of deep learning-extracted spine x-ray features to detect individuals with abnormal bone mineral density (BMD) and identify populations at high risk for osteoporosis. They found that the highest performance accuracy of 0.71 was achieved when combining feature extraction using VGG Net with classification using random forest.

K. Yasaka et al. [30] utilized CT images of the abdomen to estimate the BMD of the lumbar vertebrae using a CNN model. They found a significant correlation between the DXA bone mineral density and the predicted BMD from convolutional neural networks.

Usman et al. [31] conducted a study that utilizes knee x-ray images to assess and compare the performance of three robust transfer learning model algorithms, namely GoogleNet, VGG-16, and ResNet-50, in the classification of osteoporosis. The findings obtained through statistical analysis and Python analysis using sci-kit-learn indicate that the accuracy of the GoogleNet model was 90%, followed by the VGG-16 model with an accuracy of 87%, and the ResNet-50 model with an accuracy of 83%.

Insha et al. [32] conducted a study to assess and compare the diagnostic ability of different CNN architectures (ResNet-18, VggNet-16, AlexNet, and VggNet-19) in diagnosing osteoporosis using knee x-ray images. The findings revealed that AlexNet obtained the highest accuracy rate of 91%, while VggNet-19 exhibited the lowest performance, achieving an accuracy of 84.2%. In general, all CNNs showcased favorable diagnostic capabilities, indicating that employing transfer learning with CNNs to diagnose osteoporosis from knee x-ray images could be an easily accessible and cost-effective diagnostic method.

3 THE PROPOSED SYSTEM

The proposed system for detecting osteoporosis based on x-ray images is shown in Figure 1. It is divided into phases 1 and 2. Each phase includes several stages: image loading from the dataset, the preprocessing stage which appropriately prepares the image by removing noise, contrast enhancement, and extracting the region of interest, and the smudging stage.

The stages mentioned are similar in phase 1 and phase 2. However, the final stage in phase 1 involves training the model on a large unlabeled x-ray dataset, whereas the final stage in phase 2 involves fine-tuning the trained model with the target dataset. All of the above will be detailed in sections 3.1, 3.2, 3.3, and 3.4.

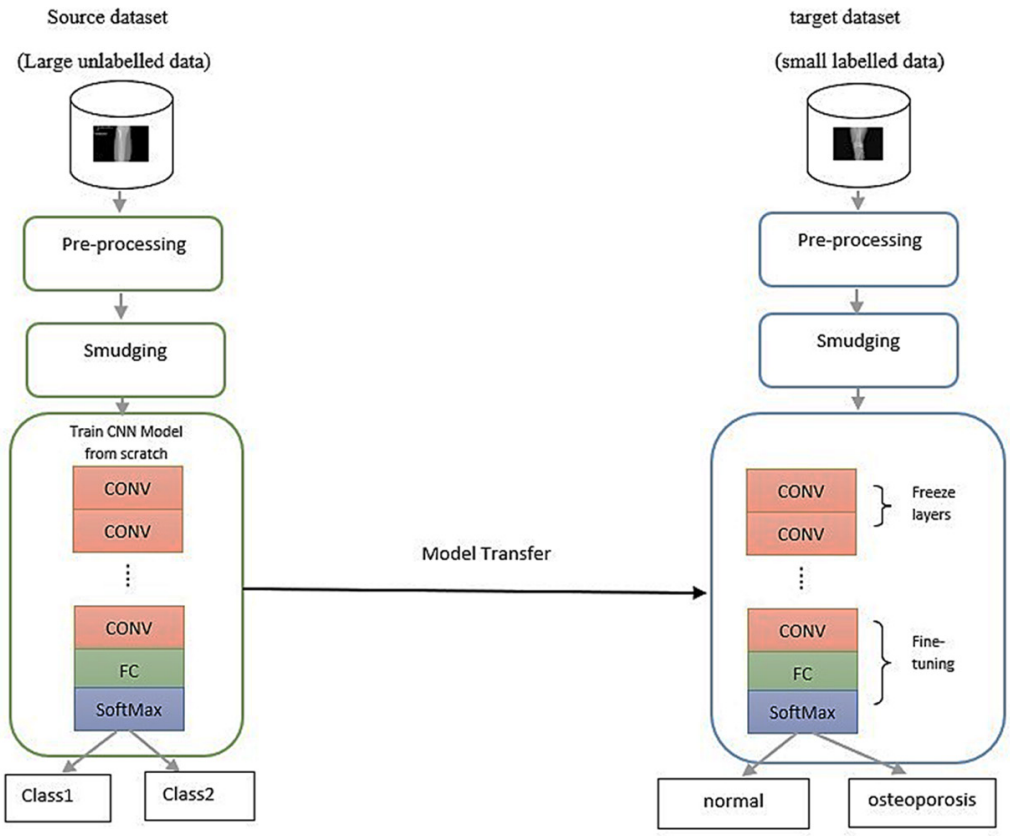

Fig. 1. The proposed system

3.1 Preprocessing

Image preprocessing refers to the techniques applied to the original image in Figure 2 to enhance its quality. This includes extracting meaningful information and making it easier to analyze and process. The benefits of image preprocessing include:

A) **Noise reduction:** Image preprocessing can remove random and coherent noise that can affect image quality and lead to inaccurate analysis. After converting the image to grayscale, a mean filter was applied to reduce noise reduction and enhance the features and details, thereby facilitating the extraction of information.

B) **Contrast enhancement:** Since the images in the database were taken under different conditions, it is necessary to improve the contrast in order to standardize the distribution of intensities. Histogram equalization is a commonly used technique for enhancing contrast. It redistributes the pixel intensities of an image to enhance its overall contrast. The fundamental concept behind histogram equalization is to distribute the pixel intensities across the complete dynamic range of the image. Figure 3 shows the enhanced image.

It is worth mentioning that contrast can be improved by deep learning, where CNN can learn to enhance the contrast in x-ray images by extracting relevant features from the input images and adjusting the pixel values accordingly.

C) **Region of interest:** Contrast enhancement is first applied to help distinguish the bones from the surrounding tissue. Applying "Thresholding" to create a binary mask that separates the bone from the background. Use morphological operations, such as erosion, to remove noise and fill in small holes in the mask.

To identify the connected components in the mask and measure their properties. The component with the largest area is likely to correspond to the bone. Extract the bone region of interest (ROI) from the original image using the mask and "region-props" function. This function returns measurements for a set of properties for each 8-connected component (object) in the binary image. By using this function, we can find the bounding box of the bone, as shown in Figure 4. Finally, the crop ROI is based on the bounding box coordinates, as shown in Figure 5.

3.2 Smudging

Smudging is a technique used in remote sensing to enhance visual representation of a map based on the content of the image. For example, agricultural areas are assigned a green color, even if they are separate, while water is given a blue or cyan color, and so on.

Since the x-ray images were collected from different individuals and under varying circumstances, the fragility area and its size differ among the images in the database. To ensure that the fragility area in the images was nearly identical and easy to differentiate, we utilized the smudging process. This involved combining the small, scattered, and converging areas to form clusters using a filter with a large window size as shown in Figure 6.

Fig. 2. Source x-ray image

Fig. 3. The enhanced image

Fig. 4. Object edge, which used as a coordinate for ROI cropping

Fig. 5. The region of interest

Fig. 6. Smudge image using a mean filter with large win-size

3.3 Proposed deep convolutional neural network

A DCNN is a type of artificial neural network specifically designed for image recognition and analysis. It is a type of deep learning model composed of multiple layers of interconnected artificial neurons that are trained to recognize patterns in image data. The key building block of a DCNN is the convolutional layer, which performs a mathematical operation called convolution to extract features from the input image. These features are then processed through multiple layers of artificial neurons, with each layer learning increasingly complex representations of the image data. The final layer of the network is typically a fully connected layer that generates the final prediction or classification. DCNNs have proven to be highly effective for image classification and object recognition tasks, surpassing traditional computer vision techniques in terms of accuracy and efficiency. They are widely used in various applications, including image classification, object detection, image segmentation, and facial recognition. Figure 7 shows the main diagram of the proposed model, which consists of 55 layers and is learnable at 40.7k. This model was designed to capture both general features and small details by controlling the size of the filter in the convolutional layer. If the size of the filter is small, it will capture the fine details, whereas a large filter will provide a more general overview. In other words, the small filter focuses on subtle features, while the large filter focuses on connecting small adjacent areas.

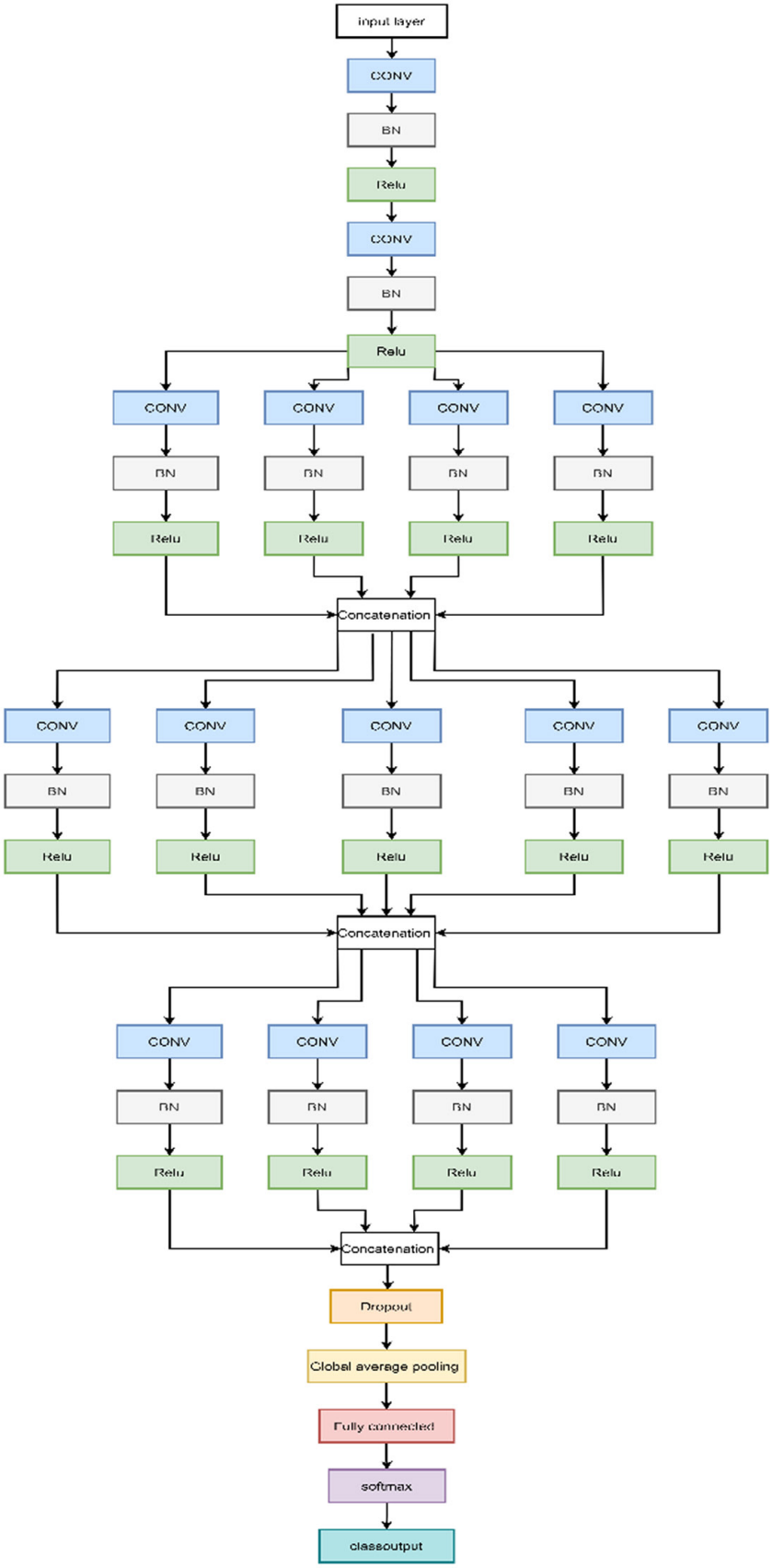

Fig. 7. The proposed model diagram

Table 1 presents the proposed DCNN model. The parameters of each layer in the proposed model are presented in Table 1. It is worth noting that CONV stands for convolutional layer, BN stands for batch normalization, and RelU stands for rectified linear unit.

Table 1. Proposed layers with their parameters

Layer	Parameters	Layer	Parameters
Input layer	[224 ×224 ×3]	CONV	3×3,32, stride 1
CONV	3×3,8, stride 1	BN	Default
BN	Default	RleU	'name', r23
RleU	Default	Block 2	Branch 4
CONV	3×3,8, stride 1	CONV	5×5,32, stride 1
BN	Default	BN	Default
RleU	'name', r1	RleU	'name', r24
Block 1	Branch 1	Block 2	Branch 5
CONV	1×1,8, stride 1	CONV	7×7,32, stride 1
BN	Default	BN	Default
RleU	'name', r11	RleU	'name', r25
Block 1	Branch 2	concatenation	5 input, the layers: r21,r22,r23,r24,r25
CONV	3×3,8, stride 1	Block 3	Branch 1
BN	Default	CONV	1×1,64, stride 1
RleU	'name', r12	BN	Default
Block 1	Branch 3	RleU	'name', r31
CONV	5×5,8, stride 1	Block 3	Branch 2
BN	Default	CONV	3×3,64, stride 1
RleU	'name', r13	BN	Default
Block 1	Branch 4	RleU	'name', r32
CONV	7×7,8, stride 1	Block 3	Branch 3
BN	Default	CONV	5×5,64, stride 1
RleU	'name', r14	BN	Default
Concatenation	4 input, the layers: r11,r12,r13,r14, 'name','cont1'	RleU	'name', r33
Block 2	Branch 1	Block 3	Branch 4
CONV	1×1,32, stride 1	CONV	7×7,64, stride 1
BN	Default	BN	Default
RleU	'name', r21	RleU	'name', r34
Layer	Parameters	concatenation	4 input, the layers: r31,r32,r33,r34
Block 2	Branch 2	Dropout	0.5
CONV	3×3,32, stride 1	Global average pooling	Default
BN	Default	Fully connected	2
RleU	'name', r22	SoftMax	
Block 2	Branch 3	Classoutput	

3.4 Transfer learning

In traditional machine learning, models are trained from scratch using a specific dataset for a particular task. Transfer learning, however, allows us to leverage of pre-existing knowledge captured by models trained on large-scale datasets. A model is trained on a large dataset for a related task within the same domain; the author collects this dataset. This pre-training step helps the model learn generic features that can be useful for various tasks.

Fine-tuning is the process of adapting or adjusting a pre-trained model using a smaller dataset that is specific to a particular task. This dataset may have different labels or slightly different characteristics compared to the original pre-training dataset. Fine-tuning was applied separately to two datasets of knee osteoporosis. During the process of fine-tuning, the parameters of the pre-trained model are adjusted to suit the specific task, while the acquired representations are retained.

By leveraging transfer learning, the following can be achieved:

Cost reduction: Training a deep learning model from scratch requires a significant amount of labeled data, computational resources, and time. Transfer learning, however, offers the advantage of utilizing existing models, eliminating the need for extensive training from scratch. As a result, this significantly reduces the overall cost associated with data collection and computational requirements.

Accelerated diagnosis: Traditional methods of diagnosing osteoporosis often involve manual interpretation of medical images by radiologists, which can be a time-consuming process. By utilizing transfer learning, the pre-trained model can quickly analyze and categorize medical images, offering an automated and efficient diagnosis. This enables faster turnaround times for diagnosis, leading to earlier interventions and improved patient outcomes.

To improve the application of transfer learning in the diagnosis of osteoporosis and assist healthcare providers in making accurate diagnoses, it is crucial to consider both technical and domain-specific factors. Here are some key strategies to improve transfer learning in this context:

Acquisition of labeled data: To obtain an accurately labeled dataset comprising bone images, which includes both healthy and osteoporotic samples, it is important to include a diverse range of demographics, age groups, and bone regions. This will ensure the robustness of the dataset.

Feature extraction: Utilize pre-trained models, such as CNNs, to extract relevant features from the bone images. These features should effectively capture significant patterns and characteristics that are indicative of osteoporosis.

Fine-tuning: Refine the pre-trained models by fine-tuning them using the labeled osteoporosis dataset. This process involves training the model on the new dataset while allowing certain pre-trained weights to be updated. Fine-tuning allows the model to adjust to the unique features and characteristics of osteoporotic bones.

Data augmentation: Employ data augmentation techniques to artificially increase the size and diversity of the osteoporosis dataset. Techniques such as rotation, scaling, flipping, and noise injection can enhance the model's ability to generalize and handle variations encountered in real-world scenarios.

Continuous learning and adaptation: Regularly update the transfer learning model when new labeled data becomes available. This iterative learning process ensures that the model remains up-to-date and maintains its accuracy as our understanding of osteoporosis and diagnostic techniques progresses.

By combining these approaches, transfer learning can significantly enhance the accuracy and efficiency of diagnosing osteoporosis. This, in turn, provides valuable support to healthcare providers in delivering optimal care to patients.

When utilizing transfer learning for the diagnosis of osteoporosis through x-rays, there are various ethical concerns and challenges that must to be taken into account. These include privacy and data security, bias and fairness, and regulatory compliance.

Transfer learning is a powerful technique in the field of machine learning that enables models trained on one task to be applied to another related task. When it comes to diagnosing osteoporosis using x-rays, transfer learning can offer several benefits, including limited data, feature extraction, and reduced training time. Limitations of transfer learning in diagnosing osteoporosis using x-rays include domain adaptation and noise in pre-trained models.

4 DATASET

Dataset A: The osteoporosis knee x-ray dataset consists of two classes: normal and osteoporosis. It was uploaded to the Kaggle dataset by STEVE PYTHON [31].

Dataset B: The knee x-ray osteoporosis database incorporates three classes (normal, osteopenia, and osteoporosis) obtained from the quantitative ultrasound system and knee x-ray for each participant. The database was uploaded on Mendeley by Insha Majeed Wani in 2021 [32].

A large unlabeled dataset: X-ray images were collected by the author from several centers (Medical City Health department/Radiology Institute, Orthopedics Specialized Center, and Raphael Hospital).

5 RESULTS

This section reviews the results obtained from the proposed system for detecting osteoporosis based on knee x-ray images in terms of accuracy, time, and error rate. Figure 8 shows the transfer learning results on the target dataset, which consists of two classes (normal and osteoporosis); each class contains 186 images. The dataset was divided into 75% for fine-tuning and 25% for testing, with a learning rate of 0.0001. Figure 9 presents the confusion matrix for the system prediction on the first dataset.

Figure 10 displays the results of transfer learning on another database for the same disease. This database consisted of three classes: normal, osteopenia, and osteoporosis. Figure 11 presents the confusion matrix for the system's prediction on the second dataset.

Tables 2 and 3 present the results obtained by the author using pre-trained classifiers, as well as results from previous studies on the same datasets.

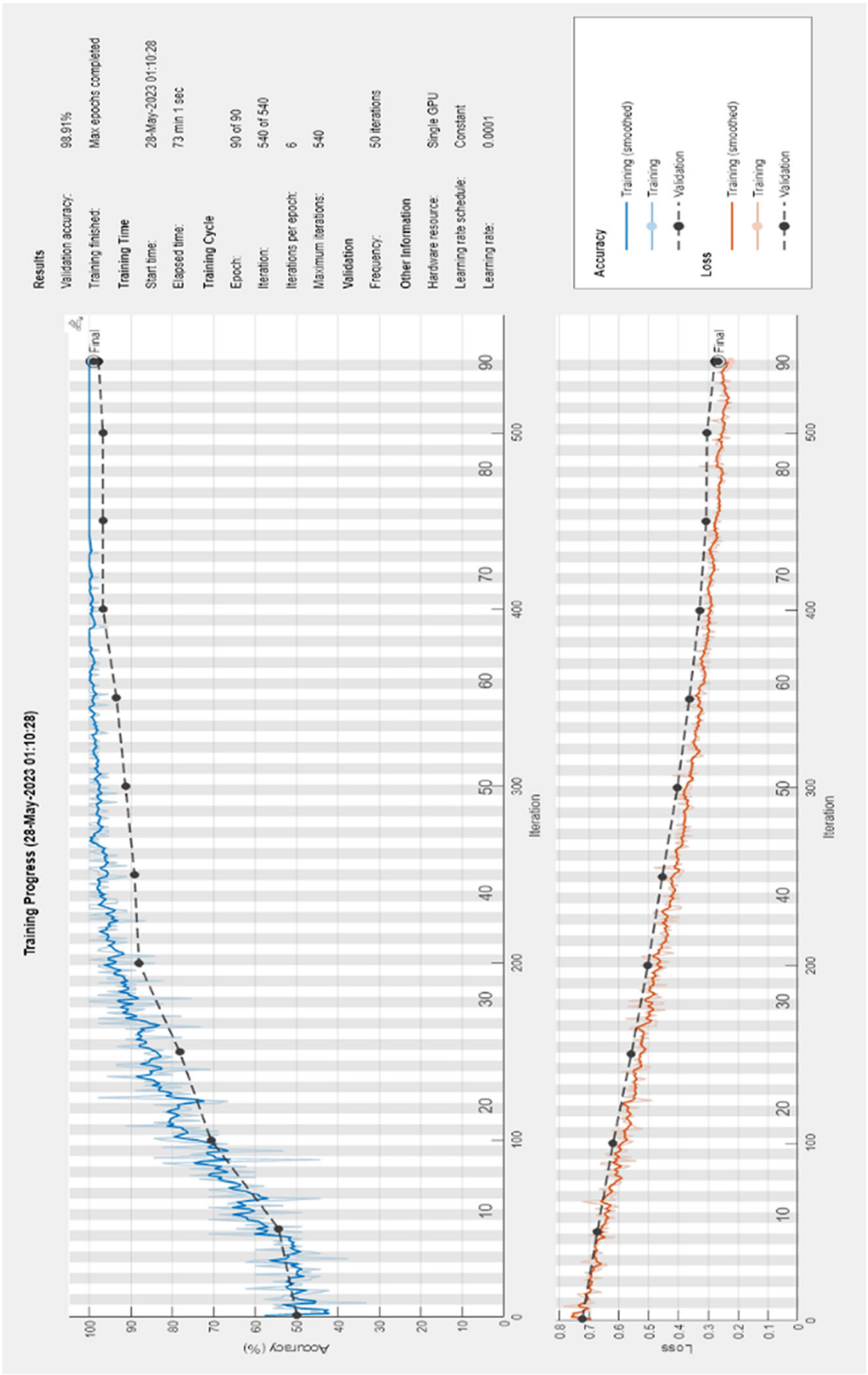

Fig. 8. Fine-tuning with the proposed model on target osteoporosis knee x-ray database (Dataset A)

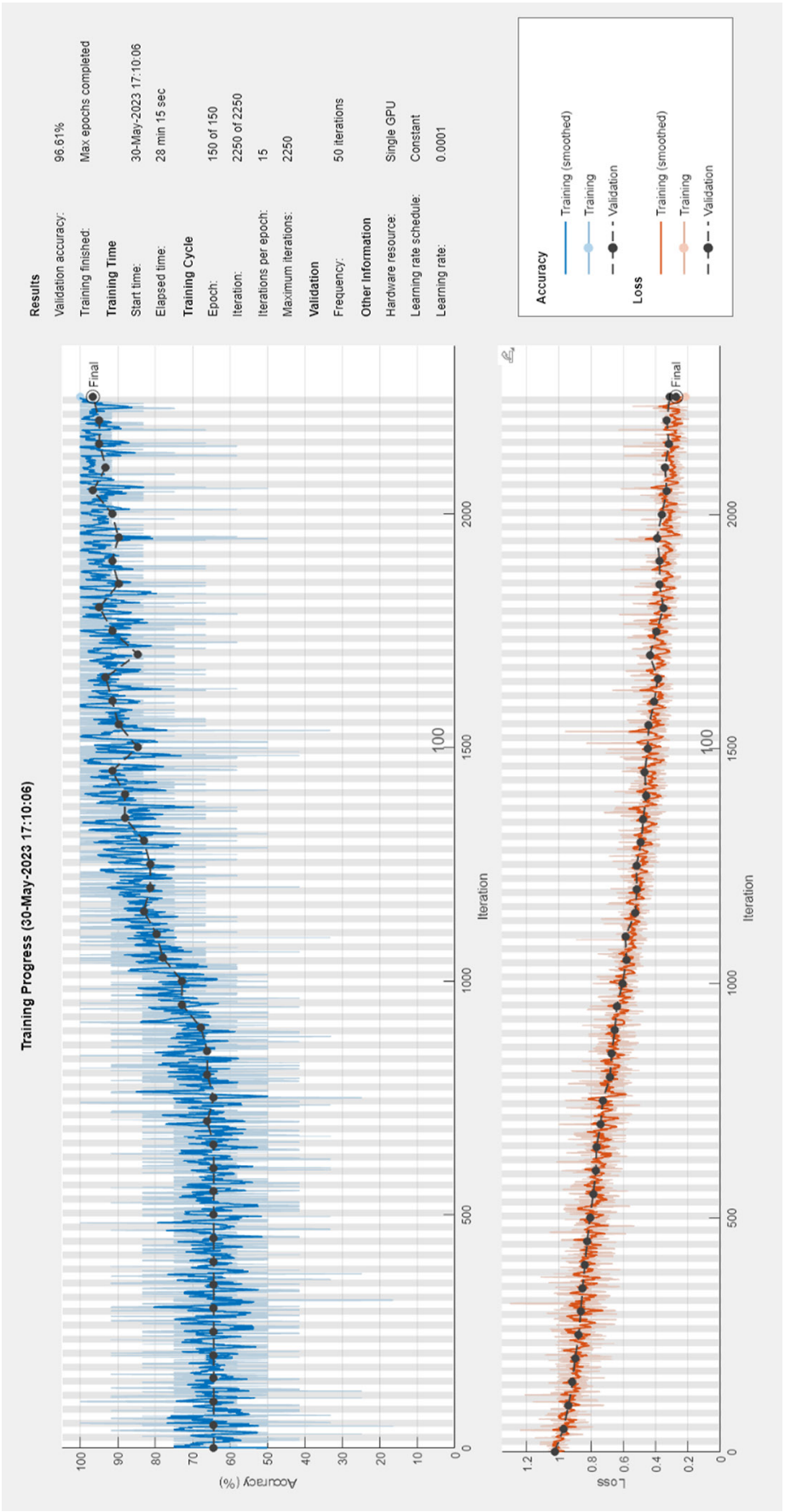

Fig. 9. Fine-tuning with the proposed model on target knee x-ray osteoporosis database (Dataset B)

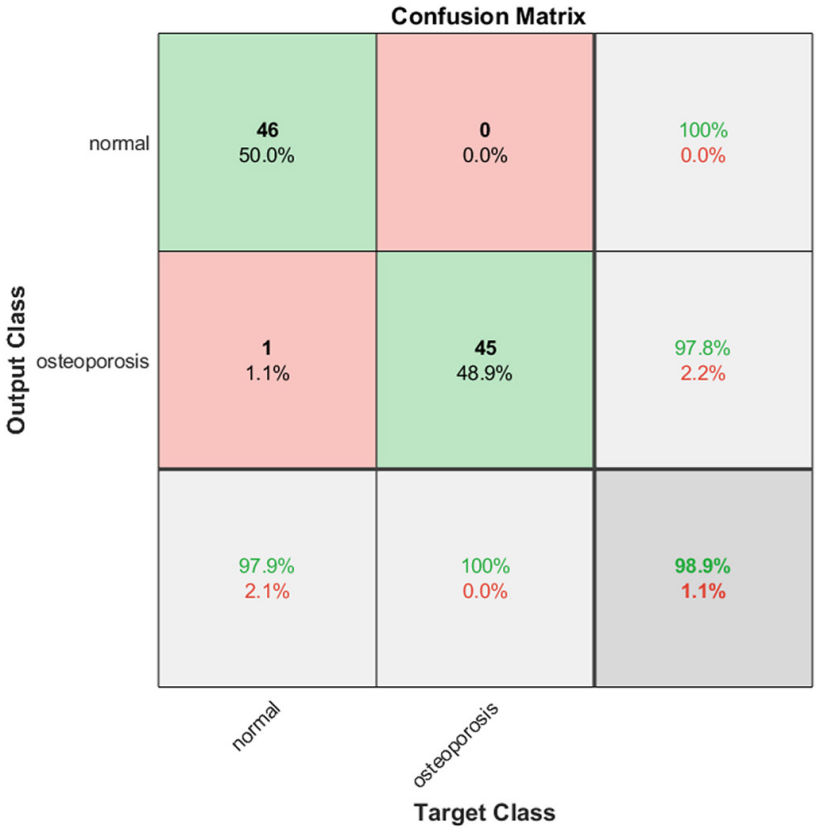

Fig. 10. The confusion matrix for system prediction on osteoporosis knee x-ray dataset (Dataset A)

Fig. 11. The confusion matrix for system prediction on knee x-ray osteoporosis dataset (Dataset B)

The accuracy is calculated according to the following:

$$accuracy = \frac{TP + TN}{TP + FP + FN + TN} \quad (1)$$

Where:

True positive (TP): The model correctly predicted an instance as "Class A" when it was actually "Class A."

False positive (FP): The model incorrectly predicted an instance as "Class A" when it was actually "Class B."

False negative (FN): The model incorrectly predicted an instance as "Class B" when it was actually "Class A."

True negative (TN): The model correctly predicted an instance as "Class B" when it was actually "Class B."

Tables 2 and 3 present the results obtained by the author using pre-trained classifiers, as well as results from previous studies on the same datasets.

Table 2. Comparison of results obtained from different models based on the osteoporosis knee x-ray dataset (Dataset A) [31]

Model	Dataset	Accuracy
Pre-trained AlexNet	Osteoporosis Knee X-ray Dataset	92.3%
Pre-trained VggNet-16	Osteoporosis Knee X-ray Dataset	89.1%
Pre-trained ResNet50	Osteoporosis Knee X-ray Dataset	90.2%
Pre-trained Xception	Osteoporosis Knee X-ray Dataset	90.2%
GoogLeNet [33] VGG-16 [33] ResNet50 [33]	Osteoporosis Knee X-ray Dataset	90% 87% 83%
Proposed model	Osteoporosis Knee X-ray Dataset	94.5%
Proposed model transfer	Osteoporosis Knee X-ray Dataset	98.91%

Table 3. The comparison of results obtained from different models based on the knee x-ray osteoporosis database (Dataset B) [32]

Model	Dataset	Accuracy
Pre-trained AlexNet	Knee X-ray Osteoporosis Database	89.8%
Pre-trained VggNet-16	Knee X-ray Osteoporosis Database	88.1%
Pre-trained ResNet50	Knee X-ray Osteoporosis Database	89.8%
Pre-trained Xception	Knee X-ray Osteoporosis Database	86.4%
AlexNet [34] VggNet-16 [34] ResNet [34] VggNet-19 [34]	Knee X-ray Osteoporosis Database	91% 86.30% 86.30% 84.20%
Proposed model	Knee X-ray Osteoporosis Database	91.5%
Proposed model transfer	Knee X-ray Osteoporosis Database	96.61%

6 CONCLUSION

In conclusion, this study has successfully addressed the challenge of detecting osteoporosis in x-ray images by employing a combination of methods, particularly through the utilization of transfer learning. The research acknowledged the importance of achieving consistency in the affected area across various images, taking into account the differences in size and location. By implementing a smudging process, the study achieved clarity in the osteoporosis-affected area, thereby facilitating the diagnosis process, particularly in the realm of image processing operations.

To develop an effective diagnostic system, multiple pre-trained CNN models were explored and evaluated. Eventually, the study introduced its own model, which showcased superior performance in detecting osteoporosis. Furthermore, the researcher encountered a scarcity of x-ray data specifically related to osteoporosis in the knee. However, this challenge was successfully overcome through the implementation of transfer learning within the same domain. By training the model on a database collected by the researcher and transferring the learned knowledge to the target database, the study achieved an impressive accuracy rate of 98.91% based on the osteoporosis knee x-ray dataset from Kaggle, surpassing the accuracy of 94% observed without the use of transfer learning in the same domain. Additionally, the study achieved an accuracy of 96.61% using the knee x-ray osteoporosis database from Mendeley data. Without utilizing model transfer in the same domain, the accuracy was 91.5%.

These findings highlight the effectiveness and potential of transfer learning overcoming data limitations and improving the accuracy of osteoporosis detection in x-ray images. The proposed system holds promise for assisting medical professionals in accurately diagnosing and monitoring osteoporosis, ultimately contributing to improved patient care and outcomes.

However, it is worth noting that further research and validation are necessary to ensure the generalizability and reliability of the proposed system. Additionally, the study opens avenues for future exploration, such as expanding the dataset and investigating the applicability of the developed model to other bone-related conditions. By continuously refining and advancing the field of osteoporosis detection through transfer learning, we can make further progress in the early diagnosis and effective management of this widespread and debilitating condition.

7 ACKNOWLEDGMENT

The author thank the Medical City Health Department/Radiology Institute, and Dr. Amer Abdulrazzaq Yaqoub in the Orthopedics Surgery Specialty Center for their assistance in obtaining databases and medical consultations.

8 REFERENCES

[1] S. Derkatch, C. Kirby, D. Kimelman, M. J. Jozani, J. M. Davidson, and W. D. Leslie, "Identification of vertebral fractures by convolutional neural networks to predict non-vertebral and hip fractures: A registry-based cohort study of dual x-ray absorptiometry," *Radiology*, vol. 293, no. 2, pp. 405–411, 2019. https://doi.org/10.1148/radiol.2019190201

[2] M. Bandirali, G. Di Leo, G. D. E. Papini, C. Messina, L. M. Sconfienza, F. M. Ulivieri, and F. Sardanelli, "A new diagnostic score to detect osteoporosis in patients undergoing lumbar spine MRI," *Eur Radiol*, vol. 25, pp. 2951–2959, 2015. https://doi.org/10.1007/s00330-015-3699-y

[3] S. R. Majumdar, J. A. Johnson, F. A. McAlister, D. Bellerose, A. S. Russell, D. A. Hanley, and B. H. Rowe, "Multifaceted intervention to improve diagnosis and treatment of osteoporosis in patients with recent wrist fracture: A randomized controlled trial," *Cmaj*, vol. 178, no. 5, pp. 569–575, 2008. https://doi.org/10.1503/cmaj.070981

[4] D. J. Becker, M. L. Kilgore, and M. A. Morrisey, "The societal burden of osteoporosis," *Curr. Rheumatol Rep*, vol. 12, pp. 186–191, 2010. https://doi.org/10.1007/s11926-010-0097-y

[5] M. A. Clynes, N. C. Harvey, E. M. Curtis, N. R. Fuggle, E. M. Dennison, and C. Cooper, "The epidemiology of osteoporosis," *Br. Med. Bull.*, vol. 133, no. 1, pp. 105–117, 2020. https://doi.org/10.1093/bmb/ldaa005

[6] M.-X. Ji and Q. Yu, "Primary osteoporosis in postmenopausal women," *Chronic Dis. Transl. Med.*, vol. 1, no. 1, pp. 9–13, 2015. https://doi.org/10.1016/j.cdtm.2015.02.006

[7] J. A. Kanis, C. Cooper, R. Rizzoli, and J.-Y. Reginster on behalf of the Scientific Advisory Board of the European Society for Clinical and Economic Aspects of Osteoporosis (ESCEO) and the Committees of Scientific Advisors and National Societies of the International Osteoporosis Foundation (IOF), "European guidance for the diagnosis and management of osteoporosis in postmenopausal women," *Osteoporosis International*, vol. 30, pp. 3–44, 2019. https://doi.org/10.1007/s00198-018-4704-5

[8] D. Hans and S. Baim, "Quantitative ultrasound (QUS) in the management of osteoporosis and assessment of fracture risk," *Journal of Clinical Densitometry*, vol. 20, no. 3, pp. 322–333, 2017. https://doi.org/10.1016/j.jocd.2017.06.018

[9] U. Ferizi, H. Besser, P. Hysi, J. Jacobs, C. S. Rajapakse, C. Chen, and G. Chang, "Artificial intelligence applied to osteoporosis: A performance comparison of machine learning algorithms in predicting fragility fractures from MRI data," *Journal of Magnetic Resonance Imaging*, vol. 49, no. 4, pp. 1029–1038, 2019. https://doi.org/10.1002/jmri.26280

[10] D. Hussain, R. A. Naqvi, W.-K. Loh, and J. Lee, "Deep learning in DXA image segmentation," *Computers, Materials & Continua*, vol. 66, no. 3, pp. 2587–2598, 2021. https://doi.org/10.32604/cmc.2021.013031

[11] H. P. Dimai, "Use of dual-energy x-ray absorptiometry (DXA) for diagnosis and fracture risk assessment; WHO-criteria, T- and Z-score, and reference databases," *Bone*, vol. 104, pp. 39–43, 2017. https://doi.org/10.1016/j.bone.2016.12.016

[12] A. D. Brett and J. K. Brown, "Quantitative computed tomography and opportunistic bone density screening by dual use of computed tomography scans," *J. Orthop. Translat.*, vol. 3, no. 4, pp. 178–184, 2015. https://doi.org/10.1016/j.jot.2015.08.006

[13] Q. F. He, H. Sun, L. Y. Shu, Y. Zhu, X. T. Xie, Y. Zhan, and C. F. Luo, "Radiographic predictors for bone mineral loss: Cortical thickness and index of the distal femur," *Bone Joint Res.*, vol. 7, no. 7, pp. 468–475, 2018. https://doi.org/10.1302/2046-3758.77.BJR-2017-0332.R1

[14] H. Jiang, C. J. Yates, A. Gorelik, A. Kale, Q. Song, and J. D. Wark, "Peripheral Quantitative Computed Tomography (pQCT) measures contribute to the understanding of bone fragility in older patients with low-trauma fracture," *Journal of Clinical Densitometry*, vol. 21, no. 1, pp. 140–147, 2018. https://doi.org/10.1016/j.jocd.2017.02.003

[15] A. Shayganfar, M. Khodayi, S. Ebrahimian, and Z. Tabrizi, "Quantitative diagnosis of osteoporosis using lumbar spine signal intensity in magnetic resonance imaging," *Br. J. Radiol.*, vol. 92, no. 1097, p. 20180774, 2019. https://doi.org/10.1259/bjr.20180774

[16] L. Wong, A. Ccopa, E. Diaz, S. Valcarcel, D. Mauricio, and V. Villoslada, "Deep learning and transfer learning methods to effectively diagnose cervical cancer from liquid-based cytology pap smear images," *International Journal of Online and Biomedical Engineering*, vol. 19, no. 4, pp. 77–93, 2023. https://doi.org/10.3991/ijoe.v19i04.37437

[17] K. A. S. H. Kumarasinghe, S. L. Kolonne, K. C. M. Fernando, and D. Meedeniya, D. "U-Net based chest x-ray segmentation with ensemble classification for covid-19 and pneumonia," *International Journal of Online and Biomedical Engineering*, vol. 18, no. 7, pp. 161–175, 2022. https://doi.org/10.3991/ijoe.v18i07.30807

[18] E. Shweikeh, J. Lu, and M. Al-Rajab, "Detection of cancer in medical images using deep learning," *International Journal of Online and Biomedical Engineering*, vol. 17, no. 14, pp. 164–171, 2021. https://doi.org/10.3991/ijoe.v17i14.27349

[19] L. Alzubaidi, M. Al-Amidie, A. Al-Asadi, A. J. Humaidi, O. Al-Shamma, M. A. Fadhel, and Y. Duan, "Novel transfer learning approach for medical imaging with limited labeled data," *Cancers (Basel)*, vol. 13, no. 7, p. 1590, 2021. https://doi.org/10.3390/cancers13071590

[20] L. R. Ali, S. A. Jebur, M. M. Jahefer, and B. N. Shaker, "Employing transfer learning for diagnosing COVID-19 disease," *International Journal of Online and Biomedical Engineering*, vol. 18, no. 15, pp. 31–42, 2022. https://doi.org/10.3991/ijoe.v18i15.35761

[21] L. R. Al-Khazraji, A. R. Abbas, and A. S. Jamil, "The effect of changing targeted layers of the deep dream technique using VGG-16 model," *International Journal of Online and Biomedical Engineering*, vol. 19, no. 3, pp. 34–47, 2023. https://doi.org/10.3991/ijoe.v19i03.37235

[22] A. A. Mukhlif, B. Al-Khateeb, and M. A. Mohammed, "Incorporating a novel dual transfer learning approach for medical images," *Sensors*, vol. 23, no. 2, p. 570, 2023. https://doi.org/10.3390/s23020570

[23] S. C. Radominski, W. Bernardo, A. P. D. Paula, B. H. Albergaria, C. Moreira, C. E. Fernandes, and V. Z. Borba, "Brazilian guidelines for the diagnosis and treatment of postmenopausal osteoporosis," *Rev. Bras. Reumatol.*, vol. 57, pp. s452–s466, 2017. https://doi.org/10.1016/j.rbre.2017.07.001

[24] N. Tomita, Y. Y. Cheung, and S. Hassanpour, "Deep neural networks for automatic detection of osteoporotic vertebral fractures on CT scans," *Comput. Biol. Med.*, vol. 98, pp. 8–15, 2018. https://doi.org/10.1016/j.compbiomed.2018.05.011

[25] I. Bortone, G. F. Trotta, G. D. Cascarano, P. Regina, A. Brunetti, I. De Feudis, and V. Bevilacqua, "A supervised approach to classify the status of bone mineral density in postmenopausal women through static and dynamic baropodometry," in *International Joint Conference on Neural Networks (IJCNN)*, IEEE, pp. 1–7, 2018. https://doi.org/10.1109/IJCNN.2018.8489205

[26] J.-S. Lee, S. Adhikari, L. Liu, H.-G. Jeong, H. Kim, and S.-J. Yoon, "Osteoporosis detection in panoramic radiographs using a deep convolutional neural network-based computer-assisted diagnosis system: A preliminary study," *Dentomaxillofacial Radiology*, vol. 48, no. 1, p. 20170344, 2019. https://doi.org/10.1259/dmfr.20170344

[27] J. Liu, J. Wang, W. Ruan, C. Lin, and D. Chen, "Diagnostic and gradation model of osteoporosis based on improved deep U-Net network," *J. Med. Syst.*, vol. 44, pp. 1–7, 2020. https://doi.org/10.1007/s10916-019-1502-3

[28] N. Tecle, J. Teitel, M. R. Morris, N. Sani, D. Mitten, and W. C. Hammert, "Convolutional neural network for second metacarpal radiographic osteoporosis screening," *J. Hand Surg. Am.*, vol. 45, no. 3, pp. 175–181, 2020. https://doi.org/10.1016/j.jhsa.2019.11.019

[29] S. Lee, E. K. Choe, H. Y. Kang, J. W. Yoon, and H. S. Kim, "The exploration of feature extraction and machine learning for predicting bone density from simple spine x-ray images in a Korean population," *Skeletal Radiol.*, vol. 49, pp. 613–618, 2020. https://doi.org/10.1007/s00256-019-03342-6

[30] K. Yasaka, H. Akai, A. Kunimatsu, S. Kiryu, and O. Abe, "Prediction of bone mineral density from computed tomography: application of deep learning with a convolutional neural network," *Eur. Radiol.*, vol. 30, pp. 3549–3557, 2020. https://doi.org/10.1007/s00330-020-06677-0

[31] Kaggle, "Osteoporosis Knee X-ray Dataset," 2021. https://www.kaggle.com/datasets/stevepython/osteoporosis-knee-xray-dataset?select=osteoporosis

[32] Insha Majeed Wani, "Knee X-ray Osteoporosis Database," Mendeley Data, ver. 1, 2021. https://data.mendeley.com/datasets/fxjm8fb6mw/1

[33] U. B. Abubakar, M. M. Boukar, and S. Adeshina, "comparison of transfer learning model accuracy for osteoporosis classification on knee radiograph," in *2nd International Conference on Computing and Machine Intelligence (ICMI),* IEEE, pp. 1–5, 2022. https://doi.org/10.1109/ICMI55296.2022.9873731

[34] I. M. Wani and S. Arora, "Osteoporosis diagnosis in knee x-rays by transfer learning based on convolution neural network," *Multimedia Tools and Applications*, vol. 82, no. 9, pp. 14193–14217, 2023. https://doi.org/10.1007/s11042-022-13911-y

9 AUTHORS

Abulkareem Z. Mohammed is Ph.D. student, did B.Sc. Computer Science from Al-Anbar University, Iraq, and M.Sc. Computing from the Informatics Institute for postgraduate studies, Iraq (E-mail: phd202010550@iips.icci.edu.iq, abdulkareemzwain@gmail.com).

Loay E. George is an Assistant Professor, Ph.D. holder, and a member of the teaching staff at College of Science/Baghdad University, Iraq. Currently working as an Assistant to UoITc President for Scientific Affairs. His main research concerns are Digital Multimedia Processing; Coding (encryption, digital signature, data compression, representation); Pattern Recognition & Classification; Fast Strings Processing and Analysis; Biometrics; and Visual Based application. Disciplines: Artificial Intelligence Information Science Computer Graphics, Pattern Recognition, Digital Image Processing, Image Retrieval, Biometrical Designs Computer Programming, Data Compression, Computer Vision, Medical and Biomedical Image Processing, Image Compression, Fractals Digital Watermarking, Images Fractal Dimension Image Processing, Signal, Image, and Video Processing, Feature Extraction, and Image Data Analysis (E-mail: loayedwar57@uoitc.edu.iq, loay.e@sc.uobaghdad.edu.iq).